Journal of Pharmaceutical and Biomedical Analysis 51 (2010) 824–833

Contents lists available at ScienceDirect

Journal of Pharmaceutical and Biomedical Analysis

journal homepage: www.elsevier.com/locate/jpba

LC/MS characterization of impurities and degradation products of a potent antitumor peptidic dimer, CU201

Jennie Wang[a,*], Vidhya Krishnamoorthi[a], Euphemia Wang[a], Chun Yang[a], Diego Baptista[a], Xiaogang Wu[a], Mingtao Liu[a], Michael Gardner[b], Phyllis Elkins[b], John Hines[b], Paul Liu[c]

[a] SRI International, 333 Ravenswood Avenue, Menlo Park, CA 94025, USA
[b] RTI International, 3040 Cornwallis Road, Research Triangle Park, NC 27709, USA
[c] Pharmaceutical Resources Branch, DCTD, NCI, 6130 Executive Blvd., Bethesda, MD 20892, USA

ARTICLE INFO

Article history:
Received 14 July 2009
Received in revised form 2 October 2009
Accepted 2 October 2009
Available online 12 October 2009

Keywords:
CU201
B201
LC–MS
Impurities characterization
Peptidic dimer
Bradykinin antagonist

ABSTRACT

Compound CU201 [SUIM-(D-Arg-Arg-Pro-Hyp-Gly-Igl-Ser-D-Igl-Oic-Arg)$_2$, where SUIM = suberimidyl; Hyp = *trans*-4-hydroxyproline; Igl = α-(2-indanyl)-glycine; Oic = octahydroindole-2-carboxylic acid], is a dimeric analog of the potent bradykinin antagonist peptide B9430. It blocks the $G_{\alpha q,11}$ signal of the heterotrimeric G proteins, stimulates c-Jun kinases, and induces apoptosis in lung cancer cells with neuroendocrine features. CU201 shows potent inhibition for small-cell lung cancer cells *in vitro* (ED_{50} = 0.15 μM), as well as for small-cell lung cancer SHP-77 tumor growth in vivo. An HPLC method was developed, as part of a study supported by the National Cancer Institute's (NCI's) Rapid Access to Interventional Development (RAID) program, to assess the purity and stability of CU201. Impurities and degradation products were characterized by LC/MS. The identity of a major impurity, with 1 mass unit different from CU201, was confirmed by high resolution LC/MS and the investigation of model compounds. Susceptible linkages in the peptide chains were revealed by the degradation study.

1. Introduction

Compound CU201 [SUIM-(D-Arg-Arg-Pro-Hyp-Gly-Igl-Ser-D-Igl-Oic-Arg)$_2$, where SUIM = suberimidyl; Hyp = *trans*-4-hydroxyproline; Igl = α-(2-indanyl)-glycine; Oic = octahydroindole-2-carboxylic acid], is a dimeric analog of the potent bradykinin antagonist peptide B9430 [1–3]. The chemical structure of CU201 is shown in Fig. 1. It was found that the dimeric analog has higher potency in binding to the bradykinin (BK) receptors than the monomeric peptide B9430. The basic character of the amidine in the cross-linking element is essential for the high receptor binding activities [1].

Small cell lung cancers (SCLCs) and many nonsmall-cell lung cancers (NSCLCs) have neuroendocrine features, including the secretion of neuropeptides and expression of cell surface receptors, which together create autocrine and paracrine growth loops. In SCLC, neuropeptides bind to a family of transmembrane receptors and activate heterotrimeric G proteins consisting of $G_{\alpha q,11}$ and $G_{\alpha 12,13}$. Low levels (ca. 10 nM) of CU201 inhibit intracellular Ca^{2+} release in response to bradykinin, indicating blockage of the $G_{\alpha q,11}$ signaling pathway and resulting in inhibition of cell proliferation. CU201, however, also stimulates the $G_{\alpha 12,13}$ pathway which, in turn, induces apoptosis. CU201-induced apoptosis was frequently preceded by unique changes in apparent nuclear DNA binding and by c-Jun kinase and caspase-3 activation. The compound is termed a "biased agonist" because it inhibits proliferation signals and stimulates apoptotic signals [2]. A further study of the "biased agonist" mechanism has been reported in a recent research paper [4]. The effects of CU201 as a BK antagonist, partial agonist and anti-proliferation agent are a function of the expression and density of the BK receptors.

CU201 shows potent inhibition for small-cell lung cancer cells *in vitro* (ED_{50} = 0.15 μM) [2,5], as well as for small-cell lung cancer SHP-77 and nonsmall-cell lung cancer A549 tumor growth in vivo [6]. The significant suppression of growth of human lung cancers in athymic nude mice models when CU201 was administered by intratumoral, s.c., or i.p. routes, at a dose of 5 mg/kg/day, has been reported [6]. CU201 also inhibits head and neck squamous cell carcinoma (HNSCC) growth through interference of epidermal growth factor receptor (EGFR) signaling pathway [7]. At the concentration at which CU201 inhibits the growth of cancer cells, it has no effect on the growth of normal lung cells *in vitro*. CU201 offers the

* Corresponding author at: SRI International, Analytical Chemistry, 333 Ravenswood Avenue, Menlo Park, CA 94025, USA. Tel.: +1 650 859 2453; fax: +1 650 859 4291.
E-mail addresses: jennie.wang@sri.com (J. Wang), hines@rti.org (J. Hines), liup@dtpepn.nci.nih.gov (P. Liu).

0731-7085/$ – see front matter © 2009 Elsevier B.V. All rights reserved.
doi:10.1016/j.jpba.2009.10.004

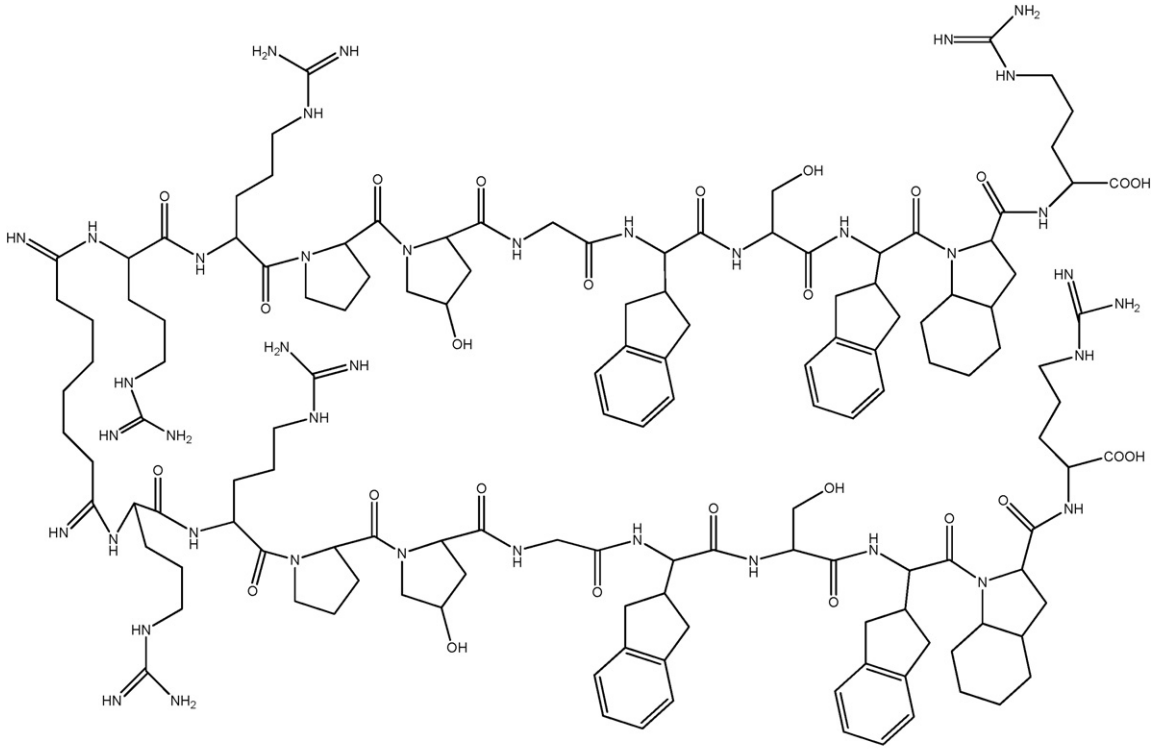

Fig. 1. Structure of CU201, SUIM-(D-Arg-Arg-Pro-Hyp-Gly-Igl-Ser-D-Igl-Oic-Arg)$_2$, where SUIM = suberimidyl; Hyp = *trans*-4-hydroxyproline; Igl = α-(2-indanyl)-glycine; Oic = octahydroindole-2-carboxylic acid.

potential of becoming a new form of targeted therapy for tumors with neuroendocrine properties [2].

As part of a study supported by the National Cancer Institute's (NCI's) Rapid Access to Interventional Development (RAID) program, an HPLC method was developed to assess the purity and stability of CU201. Impurities and degradation products were characterized by LC/MS. The identity of a major impurity, with 1 mass unit different from CU201, was confirmed by high resolution LC-Time of Flight (TOF)/MS, along with investigation of model compounds. Susceptible linkages in the peptide chains were revealed by the degradation study. Solution stability was evaluated at several pH levels.

The pharmacokinetics of CU201 in mouse was studied by Feng et al. [6,8]. Following an i.v. administration of 5 mg/kg of CU201, the kinetic profile was found to conform to a two-compartment model with an initial half-life of 14 min and a terminal half-life of 44 h. The study was conducted using a *low resolution* Finnigan LCQ ion trap mass spectrometer, with an assay based on monitoring the MS/MS transition of parent ions. The HPLC chromatogram in Feng's article, however, did not indicate the separation of CU201 from any hydrolysis degradants [8]. The apparent metabolic stability of CU201 was conflicted by a later report which disclosed that the amidine groups of CU201 spontaneously hydrolyzed in plasma within a few hours and the hydrolysis product (the suberyl derivative) was the persistent species in plasma [5]. It is likely that the reported pharmacokinetic profile was reflecting the collective level of CU201 and its hydrolysis degradants. The findings of the current study, with the aid of high resolution mass spectrometry, may warrant a re-examination of the pharmacokinetic determinations.

2. Materials and methods

2.1. Chemicals and reagents

CU201 (NSC 734868) was provided by NCI (Bethesda, MD, USA). Compound suberyl-bis-B9430 was a generous gift from Drs. L. Gera and J.M. Stewart (University of Colorado, School of Medicine, Denver, CO, USA). Formic acid (HCOOH), trifluoroacetic acid (TFA), deuterated water (D_2O), sodium deuteroxide (NaOD), and L-N^6-(1-iminoethyl) lysine hydrochloride (ImEtLys HCl) were purchased from Sigma–Aldrich (St. Louis, MO, USA). HPLC grade acetonitrile (ACN), methanol (MeOH), monobasic potassium phosphate (KH_2PO_4), sodium chloride (NaCl), and ammonium hydroxide (NH_4OH) were purchased from Mallinckrodt (Paris, KY, USA). Dibasic potassium phosphate (K_2HPO_4) was purchased from VWR International (West Chester, PA, USA). Phosphoric acid (H_3PO_4) was purchased from EMD Chemicals (Gibbstown, NJ, USA). Water was purified through a Millipore Super-Q Pure Water System (Waltham, MA, USA). For LC-TOF/MS impurity identification, reagents used were: HPLC grade ACN purchased from EMD Chemicals, Fluka ammonium formate ($HCOONH_4$) for HPLC and Reidel-de Haën formic acid, both purchased from Sigma–Aldrich, and deionized water obtained from a Picosystem UV Plus purification system (Hydro Services & Supplies, Inc., Durham, NC, USA).

2.2. HPLC

An Agilent 1100 HPLC system (Wilmington, DE, USA) equipped with a solvent degasser, quaternary pump, autosampler, and a diode array detector was used in the study. Agilent ChemStation for

LC 3D (Rev. A. 10.01) software was used for instrument operation control and data collection. The HPLC was performed on a Phenomenex Luna C8 column (3 μm, 150 mm × 4.6 mm I.D., Torrance, CA, USA). The column was held at ambient temperature (23 ± 1 °C). The mobile phase was a combination of solvent A (0.1% formic acid in water, v/v) and solvent B (0.1% formic acid in ACN, v/v). The following gradient program was used: solvent B started from 10% and linearly increased to 35% in 25 min, then returned to 10% for 10 min before the next injection. The injection volume was 5 μL. For all gradient segments, the elution flow rate was 0.5 mL/min, and the detection wavelength was set at 266 nm.

LC–MS was performed on a ThermoQuest system consisting of a Surveyor LC pump, autosampler, PDA UV detector, and a Finnigan LCQ-DUO ion trap mass spectrometer (San Jose, CA, USA). The PDA UV detector was used for recording UV–vis spectra. The mass spectrometer was equipped with an electrospray ionization (ESI) probe operating at atmospheric pressure. Positive ion mode was used, and signals in the mass range of *m*/*z* 200–2000 were collected. The LC conditions used in the LC–MS system were the same as those used in the Agilent 1100 LC-UV system.

High resolution mass spectrometry was performed on an Agilent MSD/TOF, Model G1969A, which included an Agilent 1100 HPLC system consisting of autosampler, binary pump, column heater, and diode array detector. The system used Agilent TOF software for instrument control and data acquisition and Analyst QS software for data analysis. The reversed-phase separation was performed on a HAISIL 300 C18 5 μm, 250 mm × 4.6 mm analytical column with a matching 20 mm × 3.2 mm guard column (Higgins Analytical, Inc.) at a temperature of 50 °C with UV detection at 265 nm. A 10-μL aliquot of compound dissolved in deionized water at 2.5 mg/mL was analyzed under gradient HPLC conditions. Mobile phase A was ACN/25 mM ammonium formate in water (adjusted with formic acid to pH 3.8) in 20/80 (v/v) ratio, and mobile phase B was ACN/25 mM ammonium formate in water (adjusted with formic acid to pH 3.8) in 50/50 (v/v) ratio. The linear mobile phase gradient was 20% B to 70% B in 30 min with a flow rate of 1.0 mL/min. Electrospray ionization (ESI) was used in positive ion mode. Data were acquired in a mass range of *m*/*z* 100–3200 with reference mass correction enabled.

2.3. Sample preparation

For impurity profiling, the solid samples of CU201 were dissolved in ACN/H_2O (1:1, v/v) with 0.1% of formic acid (v/v) in the solvent mixture.

The forced degradation samples were prepared by dissolving CU201 at a concentration of 0.5 mg/mL in: (1) ACN/H_2O (1:1, v/v) with 0.1% of formic acid (v/v), heated at 80 °C for 2 h; (2) H_2O, heated at 80 °C for 2 h; (3) 0.005N NH_4OH solution, kept at room temperature overnight.

The solution stability samples were prepared by dissolving CU201 at a concentration of 0.5 mg/mL in the following seven kinds of solvents: H_2O, H_2O with 0.1% formic acid (v/v), methanol, methanol with 0.1% formic acid (v/v), pH 2 phosphate buffer, pH 5 phosphate buffer, and a phosphate buffered saline (PBS) solution (pH 7.4). The phosphate buffers were made from 50 mM of KH_2PO_4, and pH was adjusted with H_3PO_4 to pH 2 and pH 5. The PBS solution was made of 10 mM K_2HPO_4, 138 mM NaCl, and 2.7 mM KCl, and then its pH was adjusted to 7.4. All the test solutions were kept at ambient temperature (23 ± 1 °C) except that the PBS solution was kept at controlled temperature at 25 and 37 °C. The test solutions were injected into the HPLC periodically to obtain the kinetic profiles.

For impurity identification, arginine free base (Arg), arginine hydrochloride (Arg HCl), and L-N^6-(1-Iminoethyl) lysine hydrochloride (ImEtLys HCl) were used as model compounds for investigation. For the LC–MS study, the three samples were dissolved individually at 1 mg/mL in H_2O. The NMR sample of ImEtLys HCl was prepared by dissolving the compound in D_2O at 1 mg/mL, and subsequently adjusted to approximately pH 6 with NaOD.

Table 1
Chromatographic purity of four lots of CU201 drug substance.

Components	C/2	C/3	S/4	S/5
CU201	81.6	76.5	79.8	76.0
MA	13.4	16.8	16.9	20.9
Other impurities	5.0	6.7	3.3	3.1

Lot C/2 and C/3 are acetic acid salts, and lot S/4 and S/5 are trifluoroacetic acid salts.

3. Results and discussion

3.1. HPLC method development

Reversed-phase HPLC (RPLC) is widely used for the analysis of peptide and protein samples [9]. A special feature of large biomolecule separation by RPLC is rapid change of retention (*k*) with change in organic solvent modifier. This behavior makes it difficult to maintain constant retention times with isocratic conditions. Gradient elution is normally required for separating peptide and protein samples. Because CU201 contains basic amino acids, low pH mobile phase is preferred to suppress residual silanol reactivity and curtail peak tailing. The low pH conditions can also prevent the formation of mixed conformation and ionization states of the peptide that would cause the appearance of multiple bands and broad or misshaped peaks. RPLC was attempted for separation of impurities and forced degradation products using C18 and C8 columns (3 μm, 150 mm × 4.6 mm, Phenomenex Torrance, CA, USA). A mixture of ACN and water was used as the mobile phase, with trifluoroacetic acid (TFA) or formic acid as mobile phase additives. In isocratic runs, the retention of CU201 varied dramatically with minute percentage changes in ACN. Gradient elution was preferred in order to obtain a reproducible retention time. Among the conditions tested, the C8 column with 0.1% formic acid in water and ACN gave the optimal separation. The gradient program was 10% to 35% ACN in 25 min, followed by equilibration at 10% for 10 min. This condition resolved a major impurity closely eluting after CU201. This major impurity amounted to approximately 15% in most drug substance batches. Several minor impurities that eluted before CU201 were well separated from the CU201 peak and the major impurity peak (Supplemental Fig. 1) under the given conditions, the HPLC was not able to separate some major degradation products. Further efforts to improve separation were not pursued because the peptide was not sufficiently pure and stable to be developed as a useful drug product (see Table 1 and discussion in Section 3.3). This HPLC method has been used to monitor the peptide's stability and to elucidate the major degradation routes by LC–MS.

3.2. Characterization of impurities and degradation products

3.2.1. Characterization of major impurities/degradation products MA and DA

Four different lots of the CU201 drug substance were analyzed using the HPLC method described above in Section 3.1. Table 1 presents the chromatographic purity results of the four lots. As shown in Table 1, there is a major impurity, labeled as MA, in all four lots varied from 13% to 21%. The total amount of other impurities varied from 3 to 7%. A representative chromatogram of lot −C/3 is provided in Supplemental Fig. 1.

Since LC parameters were compatible with MS detection, they were directly adapted to a Finnigan LCQ-DUO ion trap mass spectrometer to identify the impurities. Fig. 2 shows the LC–MS total

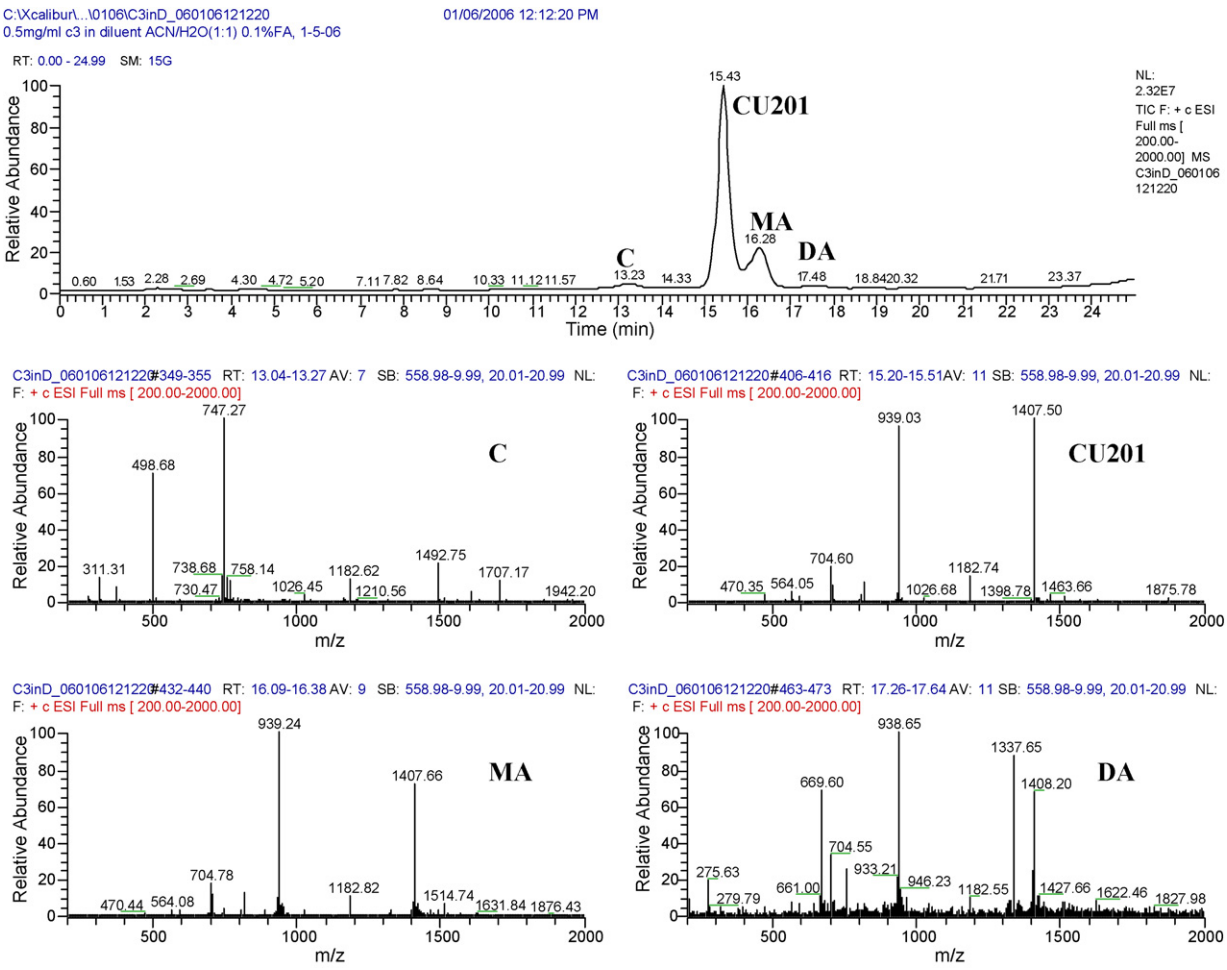

Fig. 2. TIC chromatogram (top panel) of CU201 lot –C/3, 0.5 mg/mL in ACN/H_2O (1:1) with 0.1% formic acid, fresh. The mass spectra of CU201 and impurities C, MA and DA are displayed under the chromatogram.

ion current (TIC) chromatogram and the mass spectra of CU201 and three impurities at 13.2 min (C), 16.3 min (MA), and 17.5 min (DA).

The mass spectrum of CU201 has three significant ions at *m*/*z* 1407.5, 939.0, and 704.6 (Fig. 2). Since CU201 has multiple sites that can be protonated, these ions may represent the corresponding doubly, triply, and quadruply charged precursor ions.

In order to obtain charge state information, zoom scans were subsequently performed. This high resolution scan mode for LCQ series detectors gives better mass resolution and thus can reveal the charge state of an ion. In addition, zoom scan can provide slightly better mass accuracy for multiply charged ions. The zoom scan spectra (Supplemental Fig. 2) indeed confirmed the charge state of these three ions: the mass difference between the isotopic peaks is 0.5 unit for the *m*/*z* 1407 ion, indicating that the ion had two positive charges; the mass difference between the isotopic peaks is 0.33 unit for the *m*/*z* 939 ion and 0.25 unit for the *m*/*z* 704 ion, indicating +3 and +4 charge states.

The theoretical mass of the monoisotopic molecule (A isotope) of CU201 is 2811.57, and that of the most abundant isotopic molecule

Table 2
Summary of CU201 and impurity MA zoom scan data and calculated molecular mass.

Charge state	+2	+3	+4
CU201			
Run 1	1407.16	938.41	704.08
Run 2	1407.15	938.42	704.08
Run 3	1407.10	938.38	704.05
Average	1407.14	938.40	704.07
Molecular mass calculated from the average of 3 runs	2812.27	2812.21	2812.28
Average molecular mass calculated from the 3 charge states		2812.25	
Impurity MA			
Run 1	1407.66	938.75	704.30
Run 2	1407.68	938.78	704.31
Run 3	1407.62	938.73	704.3
Average	1407.65	938.75	704.30
Molecular mass calculated from the average of 3 runs	2813.31	2813.26	2813.21
Average molecular mass calculated from the 3 charge states		2813.26	

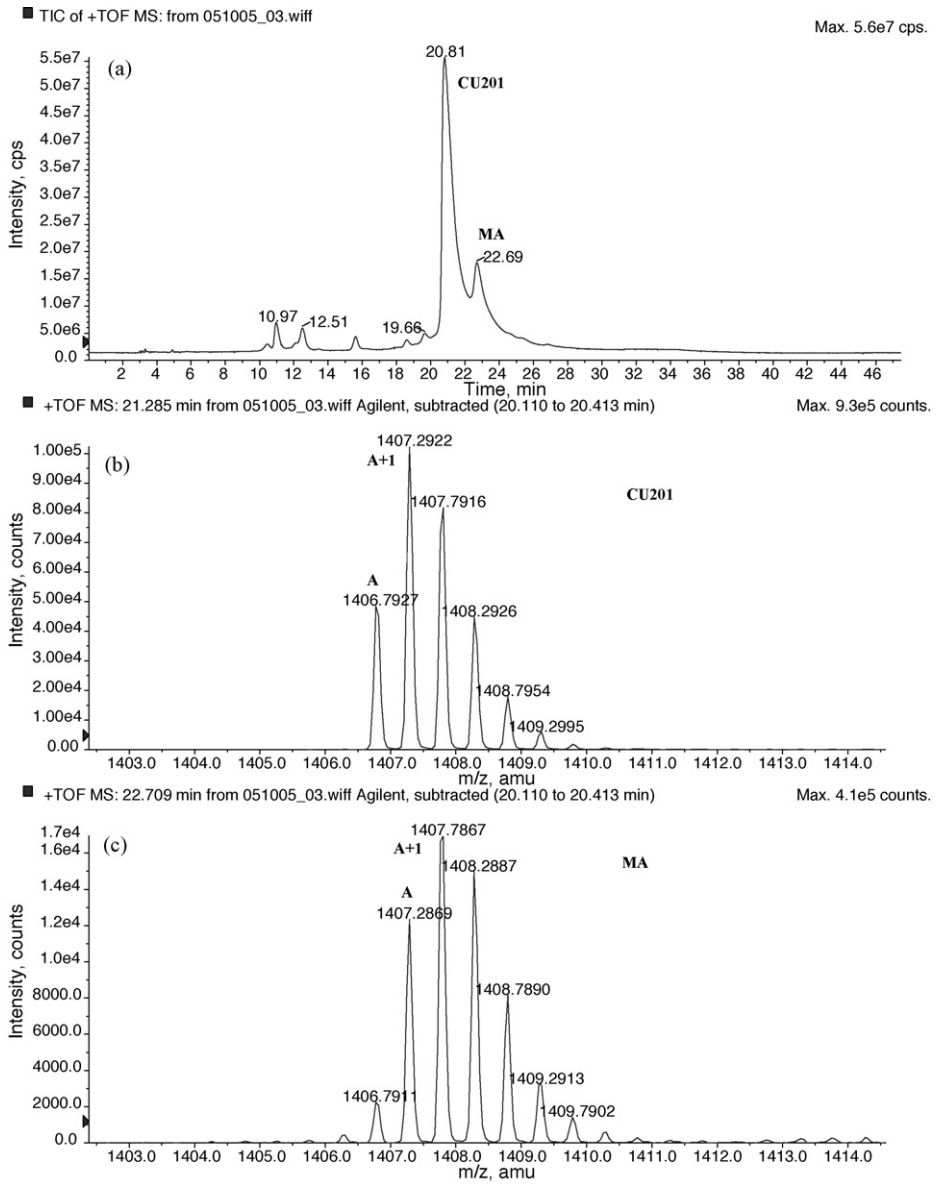

Fig. 3. (a) Total ion chromatogram (LC-TOF/MS) of CU201, lot −C/2, (b) high resolution mass spectra of the doubly charged molecular ions of major component CU201 at 20.8 min, and (c) impurity MA at 22.7 min.

(A + 1 isotope) is 2812.57. As the zoom scan spectra were obtained from a low resolution mass spectrometer, some isotopic peaks, especially at the higher charge states (i.e., +3, +4), were not well resolved. Since the most abundant isotope A + 1 would have the least interference from the adjacent peaks, it was used to calculate the molecular mass of CU201. The molecular mass values calculated from the three ions in zoom scan mode (Supplemental Fig. 2, *m*/*z* 1407.16, 938.41, and 704.08) are 2812.27, 2812.21, and 2812.28. The average value is 2812.25, which is consistent with the theoretical value of the A + 1 isotope of CU201.

The appearance of the mass spectrum of impurity MA is almost identical to that of CU201, with ions at *m*/*z* 1407.7, 939.2, and 704.8

Table 3
Summary of the high resolution mass data for CU201 and impurity MA.

Charge state	+2	+3	+4	Average
CU201 (theoretical exact mass: 2811.5714)				
Measured *m*/*z* of the monoisotopic ion	1406.7927	938.1993	703.9016	
Calculated mass	2811.5698	2811.5745	2811.5752	2811.5732
Δ calculated−theoretical (mass units)	−0.0016	0.0031	0.0038	0.0018
Δ (ppm)	−0.5691	1.1026	1.3516	0.6284
Impurity MA (theoretical exact mass: 2812.5554)				
Measured *m*/*z* of the monoisotopic ion	1407.2869	938.5296	704.1483	
Calculated mass	2812.5582	2812.5654	2812.5620	2812.5619
Δ calculated−theoretical (mass units)	0.0028	0.0100	0.0066	0.0065
Δ (ppm)	0.9955	3.5555	2.3466	2.2992

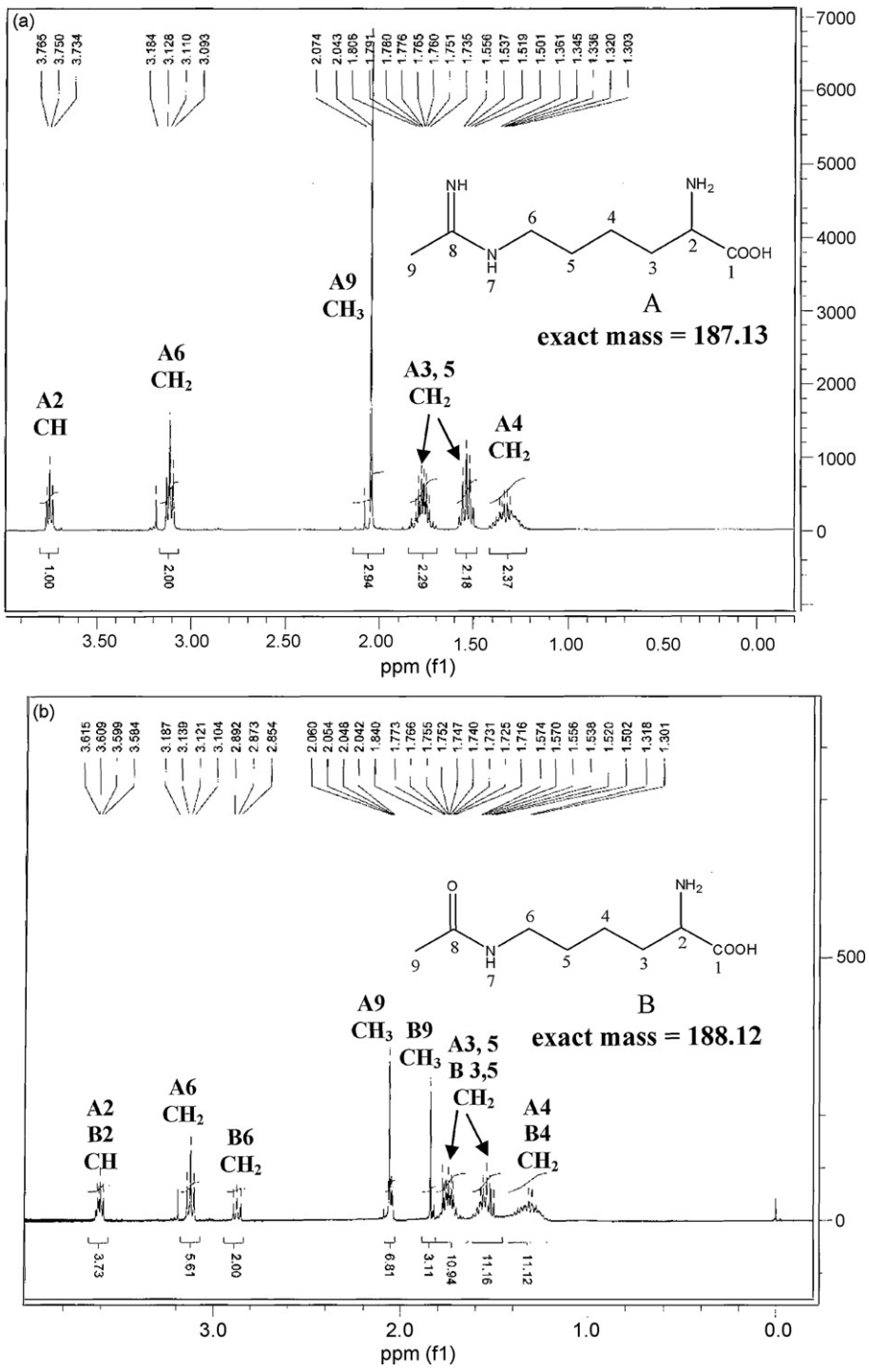

Fig. 4. ^{1}H NMR spectra of L-N^{6}-(1-iminoethyl) lysine hydrochloride (ImEtLys HCl), 1 mg/mL in D_2O. (a) 0.5 h after dissolving in D_2O and (b) 1 h after adding NaOD to adjust to pH 6.

(Fig. 2). The identity of this impurity was first suspected to be a conformer of the large peptide CU201, probably formed from the *trans*/*cis* conversion of the proline residue [10,11]. However, careful examination of the zoom scan data showed that the multiply charged ions for impurity MA were slightly but consistently higher than those for CU201. Table 2 provides a statistical summary of three zoom scan spectra data for charge states +2, +3, and +4 ions of CU201 and impurity MA. The average molecular masses calculated from multiple runs and multiple charge state ions of these two components are 2812.25 for CU201, and 2813.26 for impurity MA. These molecular masses represent the (A + 1) molecule of CU201 and impurity MA. It is apparent that the molecular mass of MA is approximately 1 mass unit higher than the mass of CU201 and plausible that one of the NH groups in CU201 has been replaced by an oxygen atom in impurity MA.

To confirm the proposed identity of MA, high resolution MS is necessary since accurate mass data would provide information on molecular compositions. Therefore, LC-TOF/MS was applied to obtain accurate measurements of the masses of CU201 and impurity MA. Fig. 3 shows the chromatogram and high resolution mass spectra of the doubly charged ions of CU201 and impurity MA. Table 3 shows the molecular masses calculated from charge states

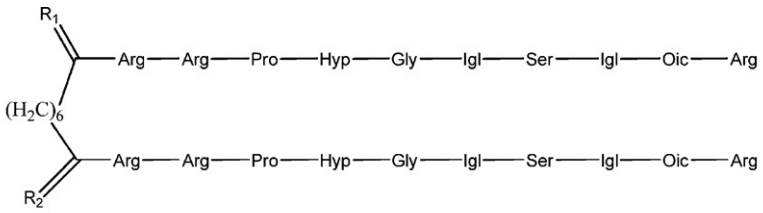

CU201: R_1 = NH; R_2 = NH, Exact Mass = 2811.57
MA: R_1 = NH; R_2 = O, Exact Mass = 2812.56
DA: R_1 = O; R_2 = O, Exact Mass = 2813.54

B, Exact Mass = 1337.74

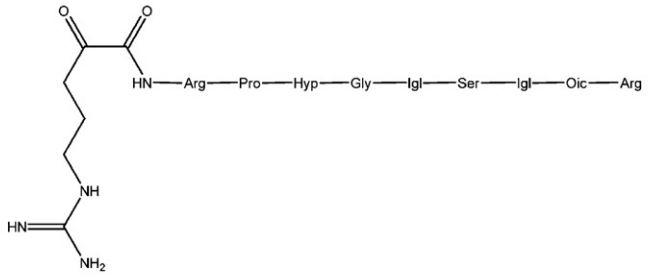

B″, Exact Mass = 1336.74

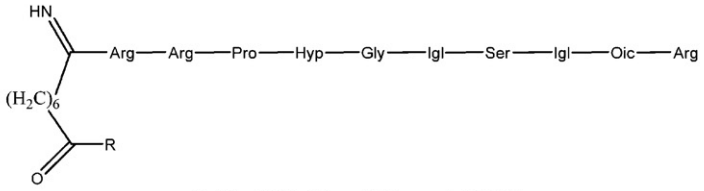

C: R = NH_2, Exact Mass = 1491.85
D: R = OH, Exact Mass = 1492.83

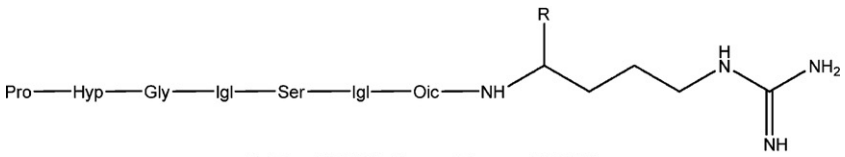

F: R = COOH, Exact Mass = 1025.53
H: R = $COOCH_3$, Exact Mass = 1039.55

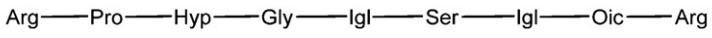

G, Exact Mass = 1181.63

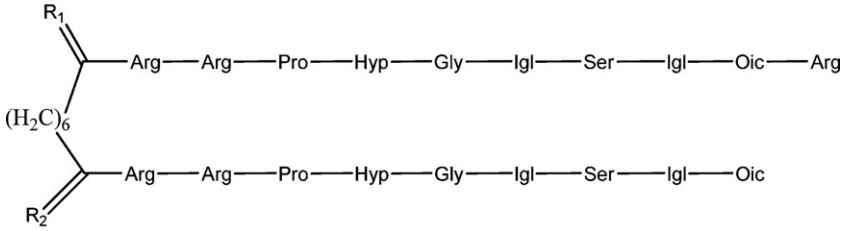

I: R_1 = NH, R_2 = O, Exact Mass = 2656.45
J: R_1 = O, R_2 = O, Exact Mass = 2657.44

Fig. 5. Proposed identities of forced degradation products.

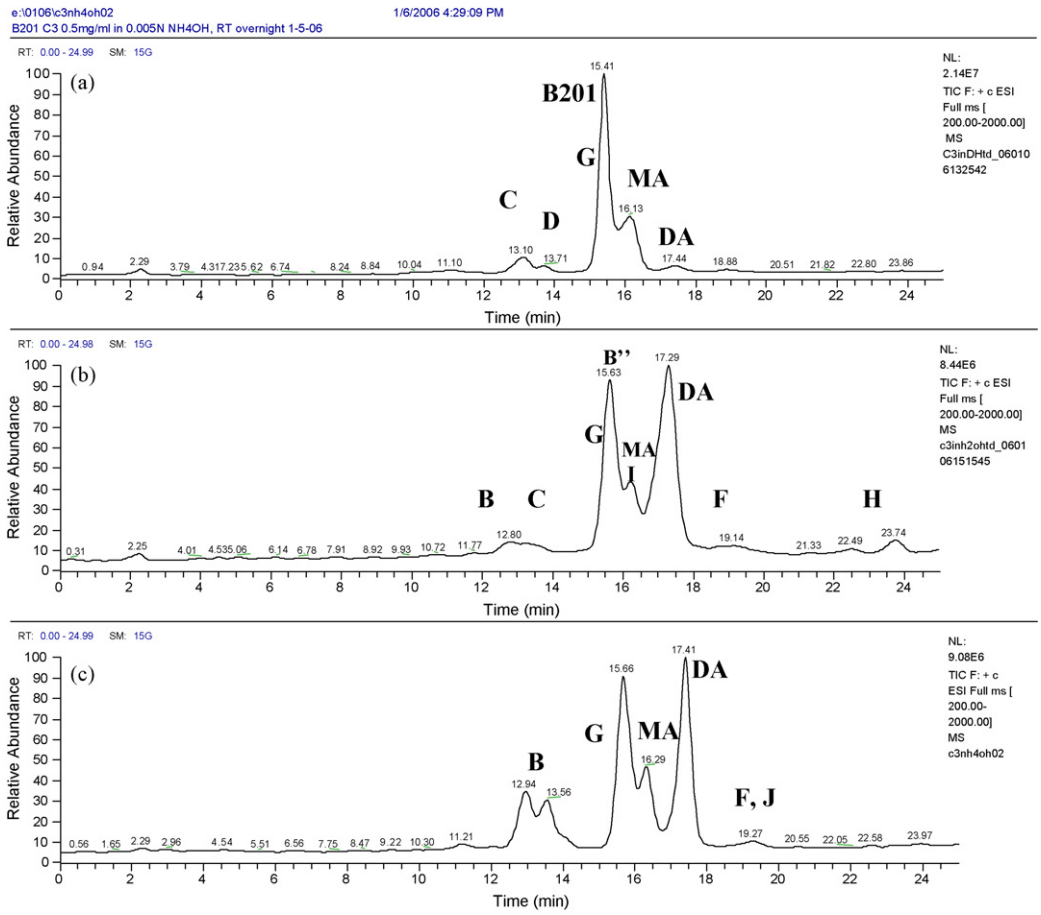

Fig. 6. TIC chromatograms of CU201, lot −C/3 forced degradation samples. (a) 0.5 mg/mL in ACN/H_2O (1:1) with 0.1% formic acid, heated at 80 °C for 2 h, (b) 0.5 mg/mL in H_2O, heated at 80 °C for 2 h, and (c) 0.5 mg/mL in 0.005 N NH_4OH, stored at room temperature overnight.

+2, +3, and +4 for CU201 and impurity MA. The average calculated mass of CU201 was 2811.5732. The deviation from its theoretical mass ($C_{136}H_{202}N_{40}O_{26}$ = 2811.5714) is 0.6 ppm. For impurity MA, the average calculated mass was 2812.5619. The deviation from the theoretical mass of the proposed molecular formula ($C_{136}H_{201}N_{39}O_{27}$ = 2812.5554) is 2.3 ppm. The accurate mass data for MA is consistent with data for the proposed molecular formula.

The molecule of CU201 (Fig. 1) has eight possible sites where the NH could be replaced by an O without cleaving the peptide chain. These sites are the two amidinyl = NH in the suberimidate bridge and the six guanidinyl = NH in the six arginine residues. As models of the amidine and guanidine structures, ImEtLys HCl, and Arg, and Arg HCl were selected for investigation. ImEtLys HCl (see structure A in Fig. 4) was dissolved in water at 1 mg/mL and monitored by LC–MS. The pH of the sample solution was 2. The compound remained unchanged after 4 h at room temperature, as shown by a single compound with the protonated molecular ion for the intact ImEtLys at *m*/*z* 188 in the LC/MS chromatogram. No other decomposition products were detected. When the solution was adjusted with base (NaOH) to pH 11, a new component with *m*/*z* 189 emerged instantly, and increased to 10% in 4 h at room temperature (LC–MS chromatograms and spectra not shown). The compound was also monitored by ^{1}H NMR on a Varian 400 (400 MHz) instrument by dissolving it in D_2O at 1 mg/mL. The solution was at approximately pH 2. The ^{1}H NMR spectrum of the D_2O solution (pH 2) is shown in Fig. 4a. The structure of ImEtLys and signal assignments are also noted on the figure. The NMR spectrum indicates that the ImEtLys is intact in the D_2O solution at pH 2. NaOD was subsequently added to adjust the pH to approximately 6, and the NMR spectrum of the solution was recorded 1 h later. New signals of the 9-CH_3 and 6-CH_2 emerged, indicating the formation of the amide component (component B in Fig. 4b). The LC–MS and NMR results demonstrate that the amidine structure is labile in mildly acidic to basic aqueous solutions (pH 6–11) and readily changes to the amide structure. However, it is reasonably stable in acidic solutions (pH 1–2).

In contrast, the guanidine structure is much more stable in both the mildly acidic and the basic aqueous solutions. The 1 mg/mL Arg HCl water solution had a pH of 6, and the 1 mg/mL Arg water solution had a pH of 9. Both solutions were stable at room temperature for at least 6 h, showing only the $[M+H]^+$ ion of Arg at *m*/*z* 175 when monitored by LC/MS. Results of the investigation of ImEtLys HCl and Arg/Arg HCl support the conclusion that the impurity MA is generated in CU201 by replacing the amidinyl =NH in the suberimidate with an oxygen (=O). The structure of MA is shown in Fig. 5.

The impurity at 17.48 min (DA in Fig. 2) has a set of multiply charged ions that correspond to 2 mass units higher than that of CU201 (Supplemental Fig. 2, zoom scan of DA). The retention time was identical to that of the authentic di-amide form of CU201 (suberyl-bis-B9430). As discussed above, the amidinyl =NH groups in the suberimidate link in CU201 are much less stable than that of the guanidine =NH groups. Subsequent forced degradation studies also indicated that DA was a significant degradation product from CU201 (Fig. 6). Therefore, DA was identified to be the degradant in which both of the amidine groups were converted to amides. The structure of DA is also shown in Fig. 5.

3.2.2. *Characterization of other degradation products*

Forced degradation was performed on the drug candidate CU201 to investigate susceptible linkages in the peptide. Fig. 6 shows the

TIC chromatogram of the forced degradation solutions. The conditions employed were acidic, neutral, and basic aqueous solutions of CU201. The full scan mass spectra of nine major degradation products are shown in Fig. 7. Although some impurities and degradation products were not well separated from each other or from CU201, they could be discerned from the mass spectra. With zoom scan to reveal the charge states of each ion, groups of ions from a single component could be easily found. For example, in the full scan spectrum of the peak at 12.9 min, ions 1338.8, 670.6, and 447.6 (Fig. 7B) could be attributed to one component, B, because their zoom scan data showed that they are in charge states of +1, +2, and +3, respectively, and their m/z values 1338.56 (Supplemental Fig. 3B), 669.69, and 446.79 (data not shown) fit in the pattern of $M+H^+$, $(M+2H^+)/2$, and $(M+3H^+)/3$. Ions 1183.0 and 592.6 could also be attributed to one component, G, for the same reason. For components with molecular mass in the range of 1000–2000, the most abundant peak is the monoisotopic peak (A), and for components with molecular mass in the range of 2000–3000, the most abundant peak is the A + 1 isotopic peak [12]. Thus, the most abundant ion observed for each component may be the A ion or the A + 1 ion, depending on the mass of the component. Determining whether an observed molecular mass represents the monoisotopic ion A or the isotopic ion A + 1 is crucial in determining the molecular formula of a degradation product. Zoom scan revealed that the singly charged molecular ions for components B, B″, G, C, H, D, and F are 1338.81, 1337.87, 1183.00, 1492.76, 1040.61, 1493.72, and 1026.58, respectively. Their molecular masses are between 1000 and 2000. Therefore the observed most abundant ions are their monoisotopic ions. Zoom scan also indicated that ions 1329.60 and 1330.17 are doubly charged for components I and J, thus their molecular masses are within the 2000–3000 range. The most abundant ions observed are their A + 1 isotopic ions. The zoom scan spectra of these nine major degradation products are shown in Supplemental Fig. 3.

Fig. 5 shows the proposed identities of major impurities and degradation products. As indicated by the degradant peak intensities (Fig. 6) and by the identities of the major degradation products, one of the labile groups in the peptide is the amidine group, which easily converted to an amide under mildly acidic to basic pH. This conversion resulted in the major impurity/degradation products MA and DA. Other susceptible linkages in CU201 are around the arginine residues. Hydrolysis between Arg and the suberimidate resulted in products B and C. Hydrolysis of the MA variant of CU201 resulted in product D. In neutral heated solution, a significant product was B″. It has a molecular mass of 1337.8, 1 mass unit less than the mass of product B. A possible formation pathway of B″ is one in which the $-C(=O)-CH(R)-NH_2$ in the Arg residue in the N-terminal is oxidized to an intermediate, $-C(=O)-C(=NH)R$, then further oxidized to a $-C(=O)-C(=O)R$ di-one structure [13]. Hydrolysis between Arg and Arg resulted in product G, and that between Arg and Pro resulted in products F and H. The Arg in the C termi-

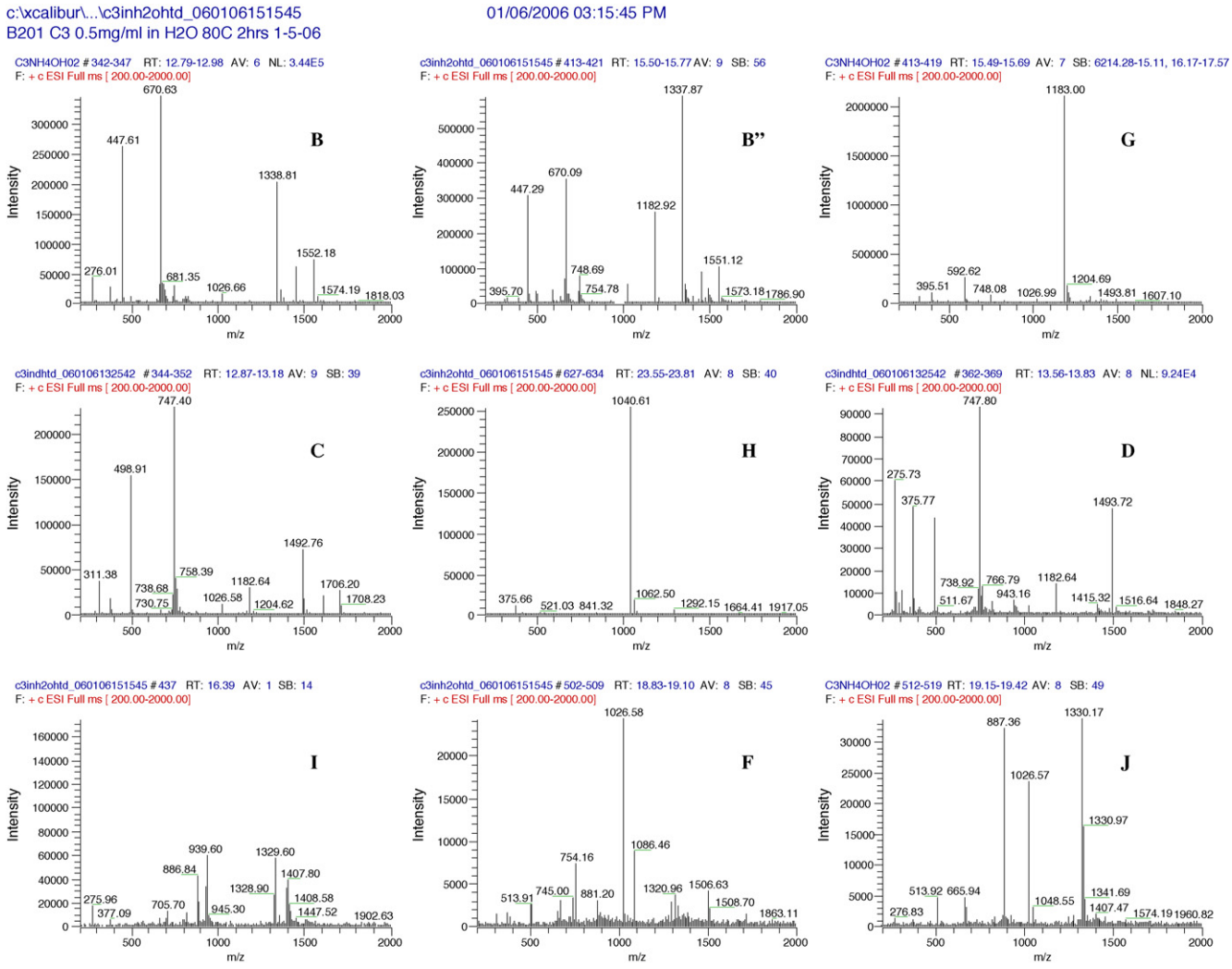

Fig. 7. Full scan mass spectra of major degradation products of CU201 lot −C/3.

Table 4
Solution stability results for CU201.

Solution	$t_{1/2}$ (h)	t_{90} (h)	First order kinetic equation coefficient r^2
Water (measured pH ~5)	31.2	1.95	0.9594
Water with 0.1% formic acid	No decay observed in 36 h		
Methanol	44.4	6.4	0.9755
Methanol with 0.1% formic acid	No decay observed in 36 h		
50 mM phosphate buffer, pH 2	No decay observed in 36 h		
50 mM phosphate buffer, pH 5	No decay observed in 36 h		
Phosphate/saline solution (PBS), pH 7.4, 25 °C	74.5	11.3	0.9671
Phosphate/saline solution (PBS), pH 7.4, 37 °C	21.8	3.3	0.9562

Sample CU201 lot −C/3 was used for the PBS solution study. Sample CU201 lot −C/2 was used for all other solution studies. All solutions were at 0.5 mg/mL. The solutions were kept at ambient temperature (23 ± 1 °C) except that the PBS solutions were controlled at 25 °C and 37 °C. The parameters $t_{1/2}$ and t_{90} were obtained from the first order kinetic model.

nal group of the peptide is also easily hydrolyzed. The detectable products I and J are derived from the MA and DA variant forms of CU201.

3.3. Solution stability

CU201 is more stable in acidic solutions than in neutral and basic solutions, as indicated by the results for the three conditions used in the forced degradation solutions (Fig. 6). In HPLC analysis for drug substance samples, CU201 was dissolved in ACN:water (1:1, v/v) with 0.1% formic acid. The solution was stable in this acidic sample diluent for at least 36 h at room temperature. To further examine the factors that affect stability, CU201 was dissolved in solvents with various pH levels, ionic strength, and aqueous/organic solvent compositions. PBS at pH 7.4 was used as the medium to simulate the in vivo environment and *iv* preparation admixture. Kinetic profiles were obtained by periodically injecting the test solution to HPLC. Table 4 shows the $t_{1/2}$ and t_{90} values of all solutions tested. (The parameters $t_{1/2}$ and t_{90} represent the amount of time required for the sample to decay 50% and 10%, respectively). The $t_{1/2}$ and t_{90} of CU201 in water are 31.2 and 1.95 h, respectively, when the pH of the solution is approximately 5. The results in Table 4 indicate that CU201 is more stable in acidic or other media with higher ionic strength. The first order kinetic plots of the PBS solution at 25 and 37 °C are presented in Supplemental Fig. 4.

The synthetic procedure for preparing the peptidic dimer CU201 involved a neutralization step, after the removal of protecting groups. Consequently, large quantities of the impurity MA (about 15% historically) were generated during the process, as a medium of pH ≤ 2 is needed to preserve the integrity of the amidine groups in CU201.

4. Conclusion

Impurities and major degradation products in CU201 drug substance were characterized by LC–MS. High resolution MS and model compounds were employed to identify the major impurity, MA. Susceptible linkages in the peptide drug were revealed from the degradation products, and conditions that affect stability were investigated. The major impurity, MA, which typically accounted for 15% of the drug substance samples, is the hydrolysis product in which the cross-linking amidine (RC(=NH)NHR′) was converted to an amide (RC(=O)NHR′). Further hydrolysis resulted in the second degradation product, DA, in which both amidine groups in the cross-linking bridge became amides. The hydrolytic lability of CU201, coupled with the unavoidable presence of high levels of impurities in the drug substance, posed an immense hurdle for drug development. The suberimidyl group, adopted to enhance activity, inadvertently contributed to the major flaw of the designed molecule.

Acknowledgements

This project has been funded with Federal funds from the Developmental Therapeutics Program, Division of Cancer Treatment and Diagnosis, National Cancer Institute, National Institutes of Health, Department of Health and Human Services, under Contract Nos. N02-CM-27134 and N02-CM-72203.

The content of this publication does not necessarily reflect the views or policies of the Department of Health and Human Services, nor does mention of trade names, commercial products, or organizations imply endorsement by the U.S. Government.

Appendix A. Supplementary data

Supplementary data associated with this article can be found, in the online version, at doi:10.1016/j.jpba.2009.10.004.

References

[1] L. Gera, J.M. Stewart, E. Whalley, M. Burkard, J.S. Zuzack, Immunopharmacology 33 (1996) 178–182.
[2] D. Chan, L. Gera, J. Stewart, B. Hekfrich, M. Verella-Garcia, G. Johnson, A. Baron, J. Yang, T. Puck, P. Bunn Jr., Proc. Natl. Acad. Sci. U.S.A. 99 (2002) 4608–4613.
[3] J.M. Stewart, L. Gera, D.C. Chan, P.A. Bunn Jr., E.J. York, V. Simkeviciene, B. Helfrich, Can. J. Physiol. Pharmacol. 80 (2002) 275–280.
[4] G. Morssette, S. Houle, L. Gera, J.M. Stewart, F. Marceau, Br. J. Pharmacol. 150 (2007) 369–379.
[5] J.M. Stewart, L. Gera, D.C. Chan, E.J. York, V. Simkeviciene, P.A. Bunn Jr., L. Taraseviciene-Stewart, Peptides 26 (2005) 1288–1291.
[6] D.C. Chan, L. Gera, J.M. Stewart, B. Helfrich, T.L. Zhao, W.Y. Feng, K.K. Chan, J.M. Covey, P. Bunn Jr., Clin. Cancer Res. 8 (2002) 1280–1287.
[7] S.M. Thomas, N.E. Bhola, Q. Zhang, S.C. Contrucci, A.L. Wentzel, M.L. Freilino, W.E. Gooding, J.M. Siegfried, D.C. Chan, J.R. Grandis, Cancer Res. 66 (2006) 11831–11839.
[8] W.Y. Feng, K.K. Chan, J.M. Covey, J. Pharm. Biomed. Anal. 28 (2002) 601–612.
[9] L.R. Snyder, J.J. Kirkland, J.L. Glajch, Practical HPLC Method Development, 2nd ed., John Wiley & Sons, Inc., 1997, pp. 497–509.
[10] E. Watson, W.C. Kenney, J. Chromatogr. 606 (1993) 165–170.
[11] W. Melander, H.J. Lin, J. Jacobsson, C. Horvath, J. Phys. Chem. 88 (1984) 4527–4536.
[12] D.H. Russell, R.D. Edmondson, J. Mass Spectrom. 32 (1997) 263–276.
[13] S. Tahara, M. Shigetsuna, H. Otomasu, Chem. Pharm. Bull. 30 (1982) 3133–3138.